Available online at www.sciencedirect.com
ScienceDirect
International Journal of Heat and Fluid Flow 28 (2007) 1405–1417
International Journal of HEAT AND FLUID FLOW
www.elsevier.com/locate/ijhff

Shroud heat transfer measurements inside a heated multiple rotating cavity with axial throughflow

C.A. Long *, P.R.N. Childs

Thermo-Fluid Mechanics Research Centre, Department of Engineering and Design, University of Sussex, Brighton, BN1 9QT, Sussex, UK

Received 27 June 2006; received in revised form 30 March 2007; accepted 2 April 2007
Available online 13 June 2007

Abstract

Experimental measurements of heat transfer are made from the inner peripheral surface of a rotating test rig designed to be similar to a gas turbine high pressure compressor internal air system. The test rig comprises a number of annular discs sealed at their periphery by a shroud. An axial throughflow of cooling air enters the test rig and flows through the annular section between the disc bores and a central shaft. Tests were carried out for the following range of rotational speeds and axial throughflow rates: $540 < N_R < 10{,}800$ rev/min and $0.124 < \dot{m} < 0.85$ kg/s (corresponding to the range of rotational and axial Reynolds numbers $4 \times 10^5 < Re_\phi < 7.7 \times 10^6$ and $3.3 \times 10^4 < Re_z < 2.2 \times 10^5$).

The shroud Nusselt numbers are found to depend on the shroud Grashof number. They are relatively insensitive to changes in axial Reynolds number and two geometrically similar cavities give similar values of Nusselt number. The heat transfer from the shroud is governed by the mechanism of free convection. It is recommended that a modified form of a correlation for Rayleigh–Bénard convection in a gravitational force field be used, with appropriate modification, to predict shroud heat transfer.

Keywords: Rotating cavity flow; Gas turbine internal air system; Axial throughflow; Shroud heat transfer; Free convection

1. Introduction

Contemporary gas turbine aircraft engines operate at the limits of technology. Gas temperatures of around 1800 K at entry to the turbine on a typical civil engine impose severe restrictions on component life. Rotational speeds of typically 10,000 rev/min on a 0.6 m diameter create significant inertial stresses. These combine with thermal stresses to create deflections in components that can cause a loss in efficiency, or worse, compromise safety.

Modern engines would not be able to operate without an internal air system. This provides ventilation (mostly cooling, but sometimes components are heated) and purging air to the discs, blades, bearing chambers and various cavities and an air supply to the seals. The source of this air is the compressor and on its route, the air may be heated by both convection and viscous dissipation. The use of internal system air is also parasitic to the main cycle, since it is bled from the compressor, where work has been done to raise its pressure. Its use may cost up to 5% of the specific fuel consumption in a modern turbofan engine (Rolls-Royce, 2005). There is therefore, a need in engine design to have knowledge of heat transfer rates and leakage flows in order to minimise the use of internal system air.

This paper is the second of two on experimental measurements of heat transfer and flow behaviour in high pressure compressor internal air systems. The objective of the work reported here was to measure the heat transfer from the inner peripheral surface, or shroud, of a test rig representative of a high pressure compressor internal air system. A background to this work is provided in Section 2, the experimental apparatus and methods of data analysis are described in Sections 3 and 4 and the results are presented in Section 5.

* Corresponding author. Tel.: +44 0 1273 678945; fax: +44 0 1273 678486.
E-mail address: c.a.long@sussex.ac.uk (C.A. Long).

0142-727X/$ - see front matter © 2007 Elsevier Inc. All rights reserved.
doi:10.1016/j.ijheatfluidflow.2007.04.009

Nomenclature

a, b	inner and outer radii, respectively
$Bi = h\ L/k$	Biot number
$Bo = Re_\phi^2 \beta \Delta T / Re_z^2$	Buoyancy number
C_p	specific heat at constant pressure
d_h	hydraulic diameter
D	rotor outer diameter
$G = s/b$	gap ratio
$Gr = \Omega^2 b \beta \Delta T L^3 / \nu^2$	Grashof number
k	thermal conductivity
L	appropriate length scale
$\dot{m}$	mass flow rate of the throughflow
N_R, N_S	rotor speed and shaft speed
$Nu = qL/\Delta T k$	Nusselt number
p	pressure
$Pr = \mu C_p / k$	Prandtl number
q	heat flux
r	radial coordinate
r_s	shaft radius
$Re_z = W d_{h/\nu}$	axial Reynolds number
$Re_\phi = \Omega\ b^2/\nu$	rotational Reynolds number
$Ro = W/\Omega a$	Rossby number
s	axial width of cavity
T	temperature
U_λ	uncertainty in the quantity λ
W	bulk mean axial velocity of the throughflow
$\beta = 1/T$	volume expansion coefficient
ΔT	temperature difference
μ	dynamic viscosity
ν	kinematic viscosity
ρ	density
$\theta = \frac{(T_{cav} - T_{in})}{(T_{sh} - T_{in})}$	cavity temperature ratio
Ω	rotational speed of the cavity

Subscripts and Superscripts

cav	pertaining to conditions inside the cavity
H	pertaining to the vertical distance between the hot and cold surfaces
i, o	pertaining to the inner and outer shroud surfaces
in	value at inlet
ref	appropriate reference value
s	denotes a value at the surface
sh	pertaining to the peripheral shroud
*	based on T_{cav}

2. Background

A review of previous work and definitions of dimensionless groups relating to the flow in rotating cavities with axial throughflow is given by Long et al. (in press). For completeness, the definitions of the dimensionless groups relevant to this current paper are repeated below. An idealised *single* rotating cavity with an axial throughflow of air comprises two discs of outer radius, b, and inner radius, a, separated by an axial gap, s. The throughflow enters the cavity through the hole $r \leqslant a$ in the upstream disc and leaves it through an identical hole in the downstream disc. The cavity is sealed at the periphery by a shroud. The rotational speed of the cavity is Ω and the bulk average velocity of the axial throughflow is W. For a fluid of kinematic viscosity, ν, the rotational and axial Reynolds numbers, Re_ϕ and Re_z, respectively, are defined as:

$$Re_\phi = \Omega b^2/\nu \tag{1}$$

$$Re_z = W d_h/\nu \tag{2}$$

where d_h is the hydraulic diameter of the inlet for a cavity with an inner shaft of radius, r_s, $d_h = 2(a - r_s)$, for one without an inner shaft, $(d_h = 2a)$. The Rossby number, Ro is defined as the ratio of the bulk mean axial velocity of the throughflow to the tangential velocity of the disc at the bore radius:

$$Ro = \frac{Re_z b^2}{2 Re_\phi a^2 (1 - r_s/a)} \tag{3}$$

Farthing et al. (1992) measured heat transfer rates from the discs of a heated rotating cavity with an axial throughflow of air, for $2 \times 10^5 \leqslant Re_\phi \leqslant 5 \times 10^6$ and $2 \times 10^4 \leqslant Re_z \leqslant 16 \times 10^4$. The cavity had a gap ratio of $G = 0.138$, $a/b \approx 0.1$, the discs were heated with either a surface temperature distribution that increased with radius or decreased with radius. The heat transfer results from the discs for a symmetrically heated cavity with a surface temperature that increased with radius suggest that the flow and heat transfer in the (narrow $G = 0.138$) cavity occurs as a result of rotationally induced laminar free convection. This finding is confirmed in the work by Long and Tucker (1994), who made heat transfer measurements (for $2 \times 10^5 < Re_\phi < 2 \times 10^6$ and $2 \times 10^3 < Re_z < 16 \times 10^4$) from the peripheral shroud of a cavity with a similar gap ratio. They found that the measured shroud Nusselt numbers were in close agreement with values predicted using an established correlation for natural convection from a horizontal surface (providing the gravitational acceleration in the usual definition of the Grashof number is replaced by the centripetal acceleration, $\Omega^2 r$, and the cavity air temperature, T_{cav}, not T_{in}, is used as the reference temperature). This is also confirmed by Long et al. (2003), who carried out measurements at higher values of Re_ϕ and Re_z in an engine representative test rig. The heat transfer from a single cavity with a wider gap ratio ($G = 0.36$, $a/b \approx 0.1$) was investigated by Long (1994). Two mechanisms were identified as being responsible for the heat transfer: rotationally induced buoyancy and the influence of the central through-

flow. Burkhardt et al. (1992) report on one of the few studies carried out on an engine representative geometry. A number of numerical studies have also been carried out and these are reviewed in Long et al. (in press). Alexiou et al. (2000) reported on the heat transfer from the disc and cone surfaces (for $10^6 < Re_\phi < 10^7$ and $3\times 10^4 < Re_z < 2\times 10^5$) in the same experimental rig as used for the work discussed in this paper. Two regimes of heat transfer were identified: for $Ro/(\beta\Delta T)^{1/2} < 6$ the heat transfer is governed by a regime of rotationally-induced free convection and for $Ro/(\beta\Delta T)^{1/2} > 6$ a regime dominated by the throughflow.

A number of more recent numerical studies (King et al., 2005 and Tian et al. (2004)) have identified the existence of pairs of cyclonic and anti-cyclonic vorticies in the flow structure. Both of these authors have noted the similarities between these and those in Rayleigh–Bénard convection that is normally associated with stationary enclosures.

3. Experimental apparatus

The heat transfer tests discussed in this paper were carried out in three different geometric configurations of a heated multiple rotating cavity test rig with axial throughflow. A full and detailed description of the rig, the instrumentation and ancillary equipment is available in the thesis by Alexiou (2000), and the reader is referred to this for further information. Alternatively, Long et al. (in press) provides a summary of the relevant details.

The test rig was operated in three different configurations which will be referred to in this paper as: (i) the disc and cone; (ii) the narrow annular gap and (iii) the wide annular gap. Fig. 1 shows a schematic diagram of the wide annular gap test rig. The rig itself is designed to be geometrically similar (approximately 70% of full size) to contemporary gas turbine aero-engines and aims to simulate internal air system flows within a high pressure compressor. The rotor is heated by a separate supply of hot air. Cooling air flows axially in the annular space between the bores and the central shaft.

For the disc and cone, the titanium 318 rotor is made up from three discs and, downstream of these, a 6 mm thick cone section, bolted together at the periphery, and having

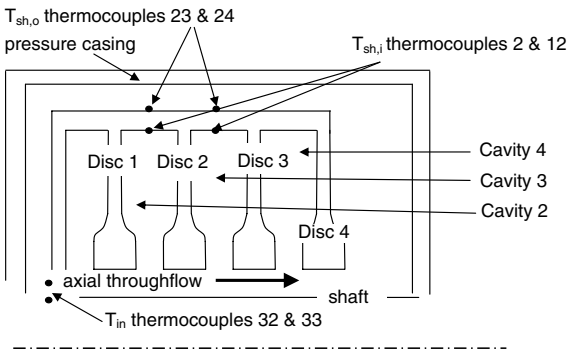

Fig. 1. The multiple cavity rig.

an outer diameter of, D. In this way the completed rotor assembly forms two cylindrical cavities and one conical cavity. Each cylindrical cavity has an outer radius of b and the axial gap ratio is $s/b = 0.195$ (dimensions have been non-dimensionalised at the request of the industrial sponsors of this project). For Disc 2, the inner radius ratio is $a/b = 0.319$ and for Disc 3, $a/b = 0.303$. The conical cavity has the same outer radius as the discs and the gap ratio varies from $s/b = 0.560$ at the inner radius to $s/b = 0.135$ at the outer radius. As in a high pressure compressor, a steel 'drive' shaft, of ($r_s/b = 0.272$) runs through the centre of the rig. This rotating shaft has twelve 15 mm diameter radial holes, equally spaced around the circumference at two axial locations towards the centre of the cone-disc cavity. This allows some of the cooling air to pass through them, the actual amount that passes through these holes is regulated (from approximately 2% of the supplied flow to 80%) by control valves on the exhaust section of the rig. The rotor and the shaft are independently driven by two separate AC motors – the rotor in one direction up to 10,000 rev/min, the shaft to 7000 rev/min in either direction.

For the narrow and wide annular gap, the cone is replaced with two titanium 318 discs (labelled in Fig. 1 as 'Disc 3' and 'Disc 4') to create four cylindrical cavities with an inner radius ratio of $a/b = 0.319$, and with a disc spacing $s/b = 0.195$. The rotating shaft is replaced by a non-rotating shaft without radial holes but with glass windows to allow optical access to the last three cavities. The difference between these two is the size of the annular gap between the disc bore and the shaft. For the narrow annular gap, this is $d_h/b = 0.092$ and in the wide annular gap, $d_h/b = 0.164$.

Air is supplied to the rig by a single stage 275 kW Howden screw compressor which can deliver up to 1.1 kg/s of air at 4 bar (absolute) and 200 °C. Before entry to the rig, the air is cooled to 30–55 °C. The air flow rate is measured by orifice plates (designed to BS 1042) at the inlet and exit to the rig. The outer surface of the rotor assembly is heated by impingement of hot air obtained from two 10 kW heaters.

The surface temperatures of the rotor assembly and relevant air temperatures are measured using 0.25 mm wire diameter K-type (NiCr–NiAl) thermocouples. The locations of these are also indicated in Fig. 1. Of particular interest are the thermocouples on the outer surface of the rotor (denoted by metal thermocouples Nos. 23 and 24) and the inner surface of the shroud (denoted by Nos. 2 and 12). The air inlet temperature is measured by air thermocouple Nos. 32 and 33. Thermal disturbance errors are reduced by the methods used to install the surface temperature thermocouples. In particular, the thermocouple bead is laid in a slot and located by deforming the edge of the slot with a small punch and using only a small quantity of ceramic cement and not epoxy resin (see Alexiou, 2000). A thermal disturbance becomes significant when the ratio of the thermal conductivity of substrate material

(in this case titanium 318) to that of the thermocouple and adhesive is much greater than unity. Turner (1970) and Long (1985) have both analysed thermal disturbance errors using a numerical solution of the conduction equation. The disturbance varies in magnitude with both the Biot number (defined using the slot dimensions and substrate thermal conductivity) and also the thermal conductivity ratio of the substrate material to that of the materials occupying the slot. For a Biot number of $Bi = 0.01$ (which corresponds to the upper range of the data presented here), a thermal disturbance of approximately 3% of the surface to fluid temperature difference would be expected from a thermal conductivity ratio of 50. For a thermal conductivity ratio of 20, the disturbance is reduced to around 1%. For a Type K thermocouple, the two constituent alloys, nickel chromium and nickel aluminium have thermal conductivities of $k = 19$ and $k = 29$ W/m K, respectively (see for example Vettori et al., 2001). For titanium 318, $k = 7.72$ W/m K, and for Sauereisen ceramic cement $k = 1.5$ W/m K. So, in the absence of any adhesive this ratio has a value of approximately 0.33 and the thermal disturbance is expected to be less than 0.1% of the surface to neighbouring fluid temperature difference. The presence of a small amount of ceramic cement will have the effect of making this ratio closer to unity and further reducing the thermal disturbance.

All the rotor instrumentation is led out to a 48-way, Wendon slip ring unit driven from the upstream side of the rig. The signals from all the temperature instrumentation are recorded by a Solartron Orion data logger, with a sensitivity of 1 μV corresponding to ±0.025 °C for the thermocouples used.

4. Experimental procedure and data analysis

The data from the heat transfer tests discussed in this paper were acquired under thermal steady state conditions. The variables investigated, their range, the corresponding range of the relevant non-dimensional groups, together with typical values from an engine, are given in Table 1. The rotational Reynolds number is defined in Eq. (1) and the kinematic viscosity, ν, is evaluated at the air reference temperature using the average of the two air inlet temperature thermocouples. The axial Reynolds number, Re_z, and the Rossby number, Ro, are defined in Eqs. (2) and (3). In the buoyancy parameter, $\beta\Delta T_{\mathrm{sh,av}}$, β and $\Delta T_{\mathrm{sh,av}}$ are the volume expansion coefficient ($\beta = 1/T_{\mathrm{in}}$), and the average shroud-surface to air-inlet temperature difference ($\Delta T_{\mathrm{sh,av}} = T_{\mathrm{sh,av}} - T_{\mathrm{in}}$). The shroud Grashof number is defined as:

$$Gr_{\mathrm{sh}} = \frac{\rho^2 \Omega^2 b \beta \Delta T_{\mathrm{sh,av}} (s/2)^3}{\mu^2} \tag{4}$$

A thermal steady state would usually take between 30 and 45 min and was confirmed by monitoring a change in surface temperatures of less than 0.2 °C in a period of

Table 1
Range of experimental conditions, values indicated in square brackets '[]' are typical of engine conditions

Parameter		Disc and cone	Narrow annular gap $d_h/b = 0.092$	Wide annular gap $d_h/b = 0.164$	Uncertainty/[]*
		Range	Range	Range	
Rotor speed	Ω (rad/s)	$158 \leqslant \Omega \leqslant 1055$	$57 \leqslant \Omega \leqslant 615$	$65 \leqslant \Omega \leqslant 608$	±1 rad/s
Cooling air flow rate	$\dot{m}$ (kg/s)	$0.12 \leqslant \dot{m} \leqslant 0.85$	$0.164 \leqslant \dot{m} \leqslant 0.80$	$0.16 \leqslant \dot{m} \leqslant 0.75$	±3%
Inlet pressure	p_{in} (bar, abs.)	$1.5 \leqslant p_{\mathrm{in}} \leqslant 3.7$	$2.2 \leqslant p_{\mathrm{in}} \leqslant 3.16$	$2.3 \leqslant p_{\mathrm{in}} \leqslant 3.7$	±0.1%
Inlet temperature	T_{in} (K)	$306 \leqslant T_{\mathrm{in}} \leqslant 328$	$309 \leqslant T_{\mathrm{in}} \leqslant 324$	$302 \leqslant T_{\mathrm{in}} \leqslant 339$	±0.2 K
Disc average surface temperature	$T_{\mathrm{s,av}}$ (K)	$320 \leqslant T_{\mathrm{s,av}} \leqslant 352$ (disc) $345 \leqslant T_{\mathrm{s,av}} \leqslant 420$ (cone)	$328 \leqslant T_{\mathrm{s,av}} \leqslant 351$	$321 \leqslant T_{\mathrm{s,av}} \leqslant 353$	±0.4 K
Shroud average surface temperature	T_{sh} (K)	$340 \leqslant T_{\mathrm{sh}} \leqslant 382$	$359 \leqslant T_{\mathrm{sh}} \leqslant 407$	$353 \leqslant T_{\mathrm{sh}} \leqslant 386$	±0.4 K
Disc rotational Reynolds number	Re_ϕ Eq. (1)	$1.1 \times 10^6 \leqslant Re_\phi \leqslant 7.7 \times 10^6$	$4 \times 10^5 \leqslant Re_\phi \leqslant 5 \times 10^6$	$4.7 \times 10^5 \leqslant Re_\phi \leqslant 5 \times 10^6$	$[8 \times 10^6]$
Axial Reynolds number	Re_z Eq. (1)	$3.3 \times 10^4 \leqslant Re_z \leqslant 2.2 \times 10^5$	$4.2 \times 10^4 \leqslant Re_z \leqslant 1.9 \times 10^5$	$4.3 \times 10^4 \leqslant Re_z \leqslant 2.0 \times 10^5$	$[2 \times 10^5]$
Rossby number	Ro Eq. (3)	$0.27 \leqslant Ro \leqslant 6.7$	$0.29 \leqslant Ro \leqslant 8.6$	$0.14 \leqslant Ro \leqslant 6.8$	[1.5]
Shroud buoyancy parameter	$\beta\Delta T_{\mathrm{av}}$	$0.07 \leqslant \beta\Delta T_{\mathrm{av}} \leqslant 0.21$	$0.14 \leqslant \beta\Delta T_{\mathrm{av}} \leqslant 0.302$	$0.086 \leqslant \beta\Delta T_{\mathrm{av}} \leqslant 0.238$	[0.35]
Shroud Grashof number	Gr_{sh} Eq. (4)	$7 \times 10^8 \leqslant Gr_{\mathrm{sh}} \leqslant 7 \times 10^9$	$3.8 \times 10^7 \leqslant Gr_{\mathrm{sh}} \leqslant 4.5 \times 10^9$	$4.0 \times 10^7 \leqslant Gr_{\mathrm{sh}} \leqslant 3.1 \times 10^9$	$[10^9]$

5 min. The measured temperatures and relevant pressures were then recorded by a computer controlled data logger and stored for future analysis. Each test comprised between 50 and 100 separate scans (each taking 1.3 s) of all the required measurements, with a delay of 2.5 s between each scan.

4.1. Heat transfer analysis

Previous experience with heat flux gauges (Farthing et al.) has demonstrated that it is not possible to rely on the manufacturer's calibration of these devices. Ideally they require calibrating in situ against a well understood flow, with abundant theoretical and experimental data for the heat transfer rate. It is obvious from the geometry of this particular test rig that this was not possible. This fact, together with the relatively small thermal disturbance from the method used to locate the thermocouples in the slots, made the use of heat flux gauges unnecessary.

The heat flux, q_{sh}, through the shroud is obtained from the one-dimensional conduction equation using measured temperatures on the inner and outer surface of the shroud $T_{sh,i}$ and $T_{sh,o}$, respectively.

$$q_{sh} = \frac{k(T_{sh,o} - T_{sh,i})}{b\ln(D/2b)} (W/m^2) \tag{5}$$

Due to the symmetry of the test rigs with the narrow and wide annular gaps, this is judged to be a good approximation. For the shroud of the disc and cone rig, this symmetry is broken and the assumption is less valid. However, the consequences of the uncertainties associated with knowing all the boundary conditions for the two-dimensional conduction solution is probably as significant as the uncertainty of assuming one-dimensional conduction. At the average temperature of the shroud, the thermal conductivity of titanium 318 is $k = 7.72$ W/m K (Touloukian et al., 1970a,b) is the cavity outer radius and D is the outer diameter of the rotor. The shroud Nusselt number, Nu_{sh}, is defined as:

$$Nu_{sh} = \frac{q_{sh}s/2}{(T_{sh,i} - T_{ref})k_{air}} \tag{6}$$

Following the use in free convection from a horizontal plate, the characteristic length scale is the ratio of exposed surface area to the perimeter, in this case half the axial gap between the discs, s/2. $T_{sh,i}$ is the surface temperature on the inside of the shroud and T_{ref} is an appropriate fluid reference temperature:

$$T_{ref} = T_{in} + \frac{\Omega^2(b^2 - a^2)}{2C_p} \tag{7}$$

The heat flux determined from Eq. (5) constitutes the total (convective and radiative) heat flux. A correction has been applied to all the data to take account of the contribution of radiative heat transfer. This uses the grey body method (see Long, 1999), using view factors obtained from the original sources quoted in Howell (1982). For an emissivity of 0.9 (which corresponds to that of black paint), the contribution of radiation is typically around 10% of the total heat flux from the shroud.

4.2. Uncertainty in the experimental measurements of heat transfer

The uncertainty in the shroud Nusselt numbers, $U_{Nu_{sh}}$, can be evaluated by partial differentiation of Eqs. (5) and (6), giving:

$$U_{Nu_{sh}} = \left\{ \left(\frac{\partial Nu}{\partial k_{Ti}} U_{k_{ti}}\right)^2 + \left(\frac{\partial Nu}{\partial T_{sh,o}} U_{T_{sh,o}}\right)^2 + \left(\frac{\partial Nu}{\partial T_{sh,i}} U_{T_{sh,i}}\right)^2 + \left(\frac{\partial Nu}{\partial s} U_s\right)^2 + \left(\frac{\partial Nu}{\partial D} U_D\right)^2 + \left(\frac{\partial Nu}{\partial b} U_b\right)^2 + \left(\frac{\partial Nu}{\partial T_{ref}} U_{Tref}\right)^2 + \left(\frac{\partial Nu}{\partial k_{air}} U_{k_{air}}\right)^2 \right\}^{1/2} \tag{8}$$

where U_λ is used to denote the individual uncertainty in a particular quantity λ.

The 95% confidence interval for the uncertainties in the measured values of shroud inner and outer surface temperatures $T_{sh,i}$, $T_{sh,o}$ is estimated to be ± 0.43 K and that for the inlet air temperature, T_{in}, is ± 0.16 K. The justification for these values is given in Table 2 and in the discussion below. The consequences of this on the uncertainty in the Nusselt numbers derived from the experimental measurements of temperature will be discussed in later sections.

The Orion data logger used to measure the signals from the thermocouples has a resolution of ± 1 μV, corresponding to ± 0.025 °C. This data acquisition system also measures the signal from the cold junction reference sensor (a solid state device with a different sensitivity to thermocouples) with a resolution of ± 10 μV corresponding to ± 0.001 °C. The main source of uncertainty in the slipring assembly will be random electrical noise. The measured values of temperatures are obtained from a statistical average of 50–100 individual measurements, and each of these individual measurements is made with an integration period of 20 ms. The calculated value of standard uncertainty for each thermocouple may then be considered to represent the uncertainty due to the rotating slipring assembly. In all cases this was less than 0.2 °C, so this value is used in Table 2.

The details of the calibration are available in the thesis by Alexiou (2000). The stability of the water bath temperature is considered to be relevant. Although the calibrated thermocouple and the PRT probe are in the same position,

Table 2
Uncertainty in thermocouple measurements

Source of uncertainty	Value ± (°C)	Probability distribution	Standard uncertainty, U_i± (°C)
Thermocouple resolution (half interval)	0.0125	Rectangular	0.0072
Cold junction resolution (half interval)	0.0005	Rectangular	0.0003
Slipring uncertainty	0.2	Normal	0.2
Calibration water bath stability	0.04167	Normal	0.04167
Calibration thermometer precision	0.015	Normal	0.015
Interpolation up to 100 °C	0.05	Normal	0.05
Repeatability	0.0415	Normal	0.0415
Combined standard uncertainty		Assumed normal	0.215 (rotating) 0.08 (non-rotating)
95% confidence interval			0.430 (rotating) 0.16 (non-rotating)

The combined standard uncertainty is given by $(\Sigma U_i^2)^{1/2}$, the 95% confidence interval is taken as twice the standard uncertainty.

the readings are not taken at exactly the same time but certainly within 5 s of each other. Based on personal experience, a temperature drift of approximately 1 °C/min can occur, (0.0833 °C in 5 s) giving an uncertainty of ±0.04167 °C.

The overall uncertainty of the Platinum Resistance Thermometer (PRT) probe and thermometer electronics, is estimated to be ±0.015 °C (Alexiou, 2000). The interpolation uncertainty and repeatability are estimated from the data given by Lancel (2002), who used similar thermocouples over a similar range of temperatures. The repeatability value is the same as quoted by Lancel, the value for the interpolation uncertainty is estimated from Lancel's data for two different ranges (±0.64 °C over the range 38–620 °C and ±0.14 °C over the range 38–280 °C). In the present measurements, the calibration is over the range 20–100 °C, which would be consistent with an interpolation uncertainty of ±0.05 °C.

The values and the associated uncertainties for all the relevant quantities in Eq. (8) are given in Table 3. These values have been used together with Eq. (8) to calculate uncertainty intervals for the shroud Nusselt number and these will be discussed in the following section. It should be noted that this excludes the uncertainty associated with any thermal disturbance. In the previous section, the upper bound to this was estimated at approximately 0.1% of the surface to fluid temperature difference. The effect of this on the Nusselt number measurements is not a random variation as is the case of the uncertainties in Table 3, but a bias. It is easy to show that the bias leads to an underestimate of the actual value of the shroud Nusselt number and has a magnitude of less than 1% of the measured value of Nusselt number.

5. Results

The variation of shroud Nusselt number with Grashof number for Cavity 2 in the narrow annular gap, $d_h/b = 0.092$, test rig is shown in Fig. 2. The shroud Grashof number, Gr_{sh} is defined in Eq. (4) by taking a conventional Grashof number and replacing the acceleration due to gravity 'g' with the centripetal acceleration at the outer radius, $\Omega^2 b$. For both Nu_{sh} and Gr_{sh}, the characteristic length scale is the cavity half-width, $s/2$, which follows from the convention of using the ratio of surface area to perimeter. Also shown for each data point is the uncertainty in the measured shroud Nusselt number obtained from the analysis described in Section 4. Typically, the uncertainty in Nu_{sh} is around ±5%. The data in this figure are grouped in similar values of the axial Reynolds number, Re_z. The shroud Nusselt number increases as the Grashof number is increased and is seen to be virtually independent of Re_z. This provides evidence that the flow mechanism responsible for the shroud heat transfer is free convection.

The values of shroud Nusselt number obtained from both Cavity 2 and Cavity 3 of the test rig with a narrow annular gap between disc bore and shaft are compared in Fig. 3. These data are for the same range of axial Reynolds numbers as shown in the previous figure. Also shown in this figure is the accepted correlation (Lloyd and Moran, 1974) for laminar ($Gr_{sh} < 10^7$) and turbulent ($Gr_{sh} > 10^7$)

Table 3
Values of uncertainty in the physical parameters relevant to the measurement of shroud heat transfer (Eqs. (5) and (6))

Quantity	Value used	Uncertainty	Source
Thermal conductivity of titanium	7.72 W/m K	±0.193 W/m K	Touloukian et al. (1970b) (Table 303)
Thermal conductivity of air	$k_{air} = (-5.289 \times 10^{-8} T^2) + (1.062 \times 10^{-4} T) - 9.7 \times 10^{-4}$ (W/m K)	Less than 1% over the range	Touloukian et al. (1970a) (Table 170)
Axial spacing between discs	s	±0.1 mm	Manufacturing tolerance
Shroud radius	b	±0.1 mm	Manufacturing tolerance
Outer diameter of rotor	D	±0.1 mm	Manufacturing tolerance
Surface temperature	$T_{sh,I}$, $T_{sh,o}$	±0.43 °C	Table 2
Air inlet temperature	T_{in}	±0.16 °C	Table 2

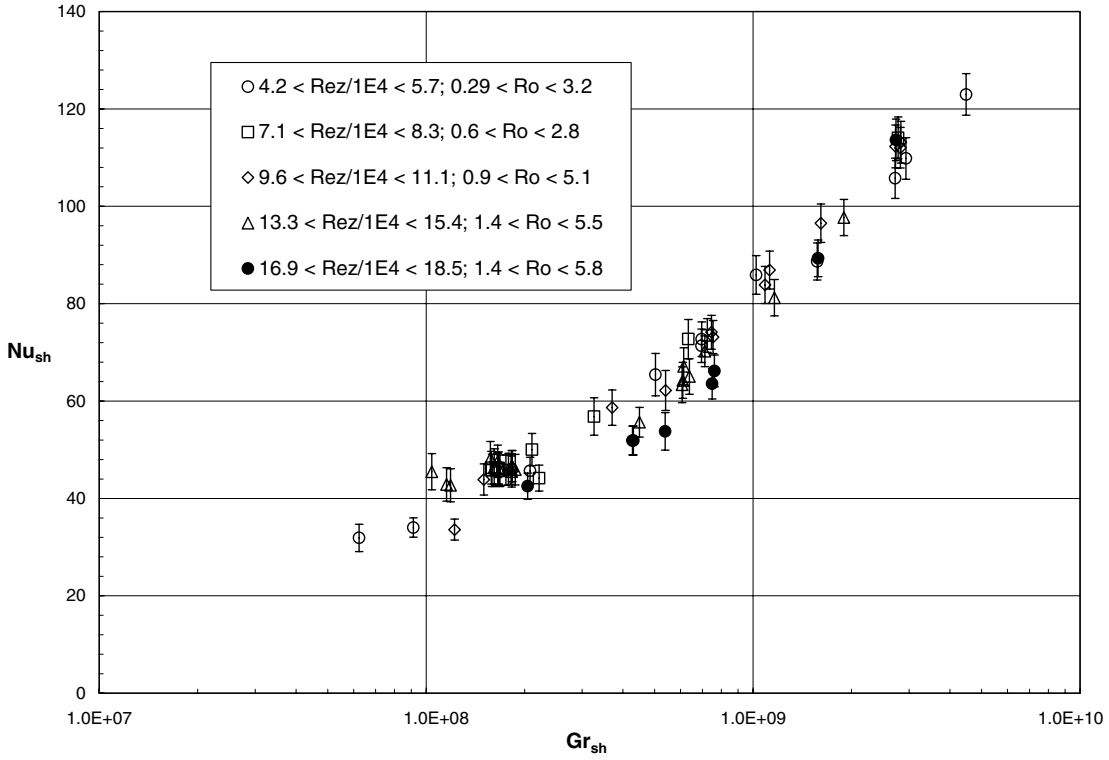

Fig. 2. Variation of shroud Nusselt number with Grashof number in Cavity 2 for $d_h/b = 0.092$ and various values of Re_z. Uncertainty bars represent values calculated using Eq. (8) and Table 3.

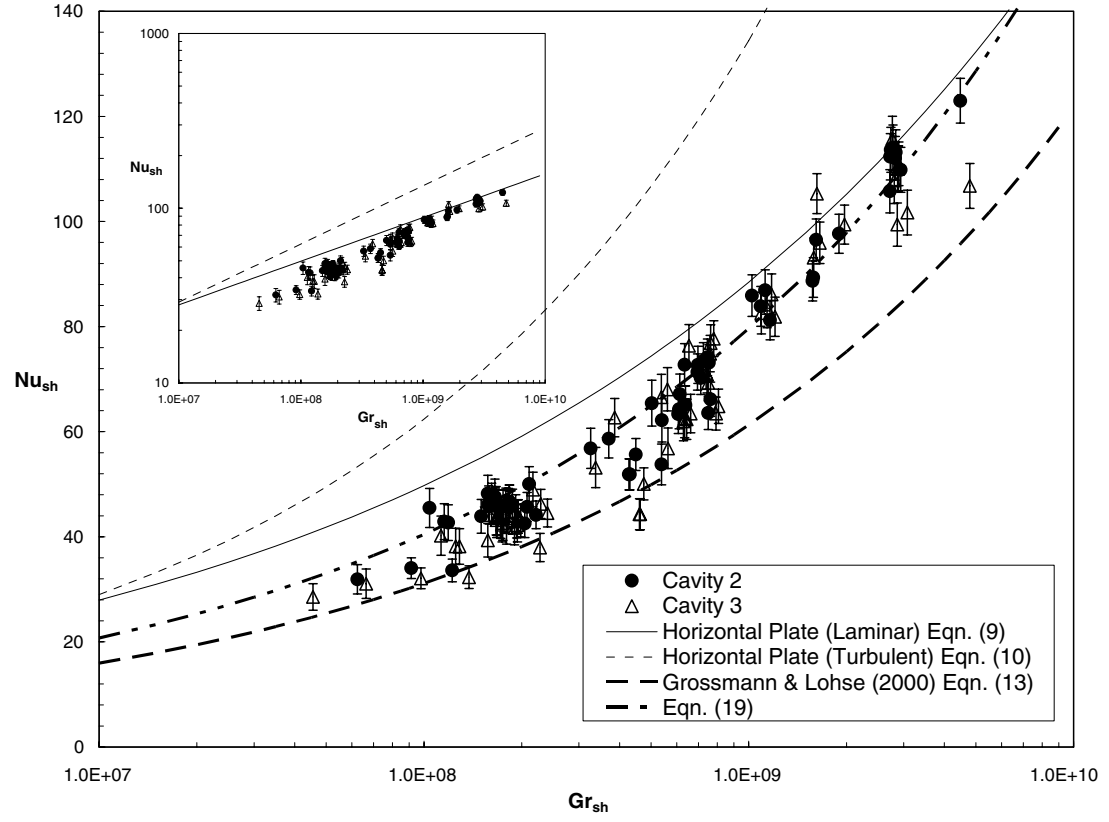

Fig. 3. Variation of shroud Nusselt number with Grashof number in both Cavity 2 and Cavity 3 for $d_h/b = 0.092$; $4.0 \times 10^4 < Re_z < 1.9 \times 10^5$; $0.29 < Ro < 5.8$. Uncertainty bars represent values calculated using Eq. (8) and Table 3. Insert is the same data plotted on a logarithmic scale.

free convection from a horizontal plate, with the upper surface heated, in a gravitational field given by:

$$\text{laminar}: Nu_{sh} = 0.54(Gr_{sh}Pr)^{1/4} \quad Gr_{sh} < 10^7 \tag{9}$$

$$\text{turbulent}: Nu_{sh} = 0.15(Gr_{sh}Pr)^{1/3} \quad Gr_{sh} > 10^7 \tag{10}$$

The growing bank of evidence (King et al., 2005; Tian et al., 2004) suggests that Rayleigh–Bénard convection may be a more appropriate mechanism to describe the flow in the outer part of an open cavity. The semi-empirical correlation of Grossmann and Lohse (2000) for Rayleigh–Bénard convection in a stationary enclosure formed by two plates separated by a vertical distance H is:

$$Nu_H = 0.27(Gr_HPr)^{1/4} + 0.038(Gr_HPr)^{1/3} \tag{11}$$

The suffix '*H*' is used to denote that the distance between the hot and cold plates H, is used as the characteristic length scale. In the current geometry, the hot surface is equivalent to the heated shroud and the cold surface the axial throughflow. In which case $H = (b - a)$ and:

$$Nu_{sh} = \left(\frac{s/b}{2(1 - a/b)}\right) Nu_H;$$

$$Gr_{sh} = \left(\frac{s/b}{2(1 - a/b)}\right)^3 Gr_H \tag{12}$$

so, with $s/b = 0.195$ and $a/b = 0.319$:

$$Nu_H = 0.166(Gr_HPr)^{1/4} + 0.038(Gr_HPr)^{1/3}. \tag{13}$$

It is worth noting that the leading constant or prefactor[1] in the second term of Eq. (11) does not change because with $Nu \propto Gr^{1/3}$ dependence the relationship is independent of length scale.

The horizontal plate correlations model the flow as external free convection. So the reference temperature used in both the Grashof and Nusselt numbers is that of a local air temperature. For a rotating cavity with an axial throughflow, this would correspond to the temperature of the air inside the cavity itself, T_{cav} and not the temperature of the inlet air, T_{in}. For Rayleigh–Bénard (internal free) convection, the temperature of the cold surface is used as the reference temperature. For a rotating cavity with a heated peripheral shroud and with axial throughflow, the cold surface is not a solid boundary but the throughflow itself. This implies that the inlet temperature can be used as the reference temperature for these correlations. For the purpose of this figure, a value of $Pr = 0.72$ was used to generate the curves for these correlations, a value which is typical of the conditions for the range of experimental data.

There does not appear to be any systematic difference between the shroud Nusselt numbers obtained from Cavity 2 and Cavity 3. This is hardly surprising since the cavities are geometrically identical. From the bulk of evidence to date it is almost certain that the heat transfer from the shroud is due to free convection. The important question that remains to be answered is how can this behaviour be best represented? It appears that the experimental data show close agreement with the correlation for laminar free convection from a horizontal surface (Eq. (9)). It is a known fact that rotation can damp out, or even prevent, turbulence. In a closed cavity (i.e. without axial throughflow), it is quite likely that this will delay the onset of turbulence beyond the accepted criterion for transition in a stationary environment (in this case $Gr_{sh} > 10^7$), or even prevent it altogether. The numerical simulations of Sun et al. (2004) have shown that this is indeed the case. The Coriolis force suppresses convection and the behaviour remains laminar at Grashof numbers where it would normally be expected to be turbulent. However, this apparently good agreement is considered to be misleading.

In an open cavity (i.e. with axial throughflow) turbulence in the throughflow may be expected to propagate into the cavity itself. So transition to turbulent free convection will occur, at perhaps a higher value of Grashof number than usually associated with stationary free convection. The LDA measurements of Long et al. do show that the axial throughflow is highly turbulent (the turbulent fluctuations are typically ±40% of the axial velocity in the inlet section and ±5% of the disc tangential velocity at the outer radius) and although it is reduced, turbulence does propagate into the cavity and the region close to the shroud. These measurements of flow behaviour would then appear to support the hypothesis that the heat transfer is associated with turbulent free convection. There is evidence of this in Fig. 3 in the log-log plot of the data shown in the insert. Although their magnitude is lower, the *gradient* of the data are closer to the curve for turbulent flow (where $Nu_{sh} \propto Gr_{sh}^{1/3}$) than it is for laminar flow (where $Nu_{sh} \propto Gr_{sh}^{1/4}$).

Long and Tucker (1994) carried out experiments on a single cavity ($a/b = 0.1$, $s/b = 0.13$) with axial throughflow but at lower values ($2 \times 10^6 < Gr_{sh} < 5 \times 10^8$) of shroud Grashof number than presented here. They also made measurements of the air temperature inside the cavity, T_{cav}, and found that if this was used, rather than the air inlet temperature, in the definition of the Grashof and Nusselt numbers, then there was good agreement with the above correlations for free convection from a horizontal plate. In their case, most of the data were in the transition region where the laminar and turbulent correlations give similar values, so it was not possible for them to identify if the flow behaviour was laminar or turbulent. For the data presented here, it was not possible to measure T_{cav}. Nonetheless, it is possible to estimate a value of T_{cav} as being the value of temperature that would occur to make the experimental data coincident with the appropriate correlation. If the values of shroud Nusselt number and Grashof number based on T_{cav} and not T_{in} are denoted by Nu^*_{sh} and Gr^*_{sh}, then:

$$Nu^*_{sh} = C(Gr^*_{sh}Pr)^n \tag{14}$$

[1] The term 'prefactor' is used in the original article by Grossmann and Lohse. It would seem to be more appropriate than the word 'constant' since as noted by the authors the numerical value of these prefactors are not universal and are therefore not expected to be constant.

where the values of C and n are given by either Eq. (9) or Eq. (10). Also, from the definitions of these non-dimensional groups, they are related by:

$$Nu^*_{sh} = Nu_{sh}\frac{T_{sh}-T_{in}}{T_{sh}-T_{cav}} \tag{15}$$

and

$$Gr^*_{sh} = Gr_{sh}\frac{T_{sh}-T_{cav}}{T_{sh}-T_{in}} \tag{16}$$

Defining a dimensionless cavity air temperature, θ, as

$$\theta = \frac{(T_{cav}-T_{in})}{(T_{sh}-T_{in})} \tag{17}$$

where a value of $\theta = 0$ implies that $T_{cav} = T_{in}$ and a value of $\theta = 1$ implies $T_{cav} = T_{sh}$. Finally, by combining Eqs. (14)–(17) it can be shown that the cavity air temperature expressed as a non-dimensional ratio is given by:

$$\theta = 1 - \left[\frac{C(Gr_{sh}Pr)^n}{Nu}\right]^{\left(\frac{-1}{n+1}\right)} \tag{18}$$

For $Gr_{sh} < 10^7$, $C = 0.54$ and $n = 1/4$ (i.e., Eq. (9)) and for $Gr_{sh} > 10^7$, $C = 0.15$ and $n = 1/3$ (i.e., Eq. (10)).

In general, the values of θ obtained from Eq. (18) are in the range $0.2 < \theta < 0.4$. This is consistent with the measurements of θ by Long and Tucker (1994) who for tests at $0.1 < Ro < 10$ with unheated discs and a heated shroud obtained values (note their definition is different to that used here but it is a simple matter to transform) of dimensionless cavity air temperature in the range $0.2 < \theta < 0.3$ and for tests with heated discs and a heated shroud in the range $0.3 < \theta < 0.4$. Calculated values of θ to achieve coincidence with Eq. (9) (laminar free convection from a horizontal plate), are much lower and than this and to achieve coincidence with Eq. (9), in most cases results in $T_{cav} \approx T_{in}$ and even $T_{cav} < T_{in}$ (which is considered to be unlikely). Since it is reasonable to assume that $T_{cav} > T_{in}$, this would appear to exclude Eq. (9). The difference between the values of θ obtained assuming laminar free convection and the measurements of Long and Tucker appear to indicate that the flow is not laminar. This, together with the fact previously noted that the data show a $Nu_{sh} \propto Gr_{sh}^{1/3}$ dependence makes it seem likely that the flow is turbulent, that the heat transfer from the shroud can be predicted by the correlation for free convection from a horizontal surface.

The above comments would tend to lead to the conclusion that Eq. (10), for turbulent flow from a horizontal plate, should be used to predict the shroud heat transfer. However, the more recent evidence for Rayleigh–Bénard convection suggests that this agreement is at best fortuitous and does not represent the physics of this flow. The correlation for Rayleigh–Bénard convection given by Grossmann and Lohse involves two prefactors. In the original form of the equation (Eq. (11)), these are 0.27 and 0.038. As acknowledged by the authors, although the exponents probably are universal, the values of prefactors are not. They are expected to depend on for example geometry or aspect ratio of the cavity. It is then, quite acceptable to change these values of prefactors until an acceptable fit is found with the experimental data. Obviously changing the two values independently of each other could lead to many possible combinations of best vales of prefactors. To simplify this, the choice of prefactors is constrained so that their ratio is constant. In this case, the most acceptable fit to the experimental data shown in Fig. 3 is given by

$$Nu_{sh} = 0.216(Gr_{sh}Pr)^{1/4} + 0.0494(Gr_{sh}Pr)^{1/3} \tag{19}$$

The variation of shroud Nusselt number with Grashof number for the test rig with the wide annular gap, $d_h/b = 0.164$ (i.e., almost twice the annular gap between disc bore and shaft) is shown in Fig. 4. The same comments as noted for the narrow annular gap are seen to still apply: Nu_{sh} is virtually independent of Re_z and only depends on the shroud Grashof number, Gr_{sh}; there is no significant difference between the shroud Nusselt numbers from Cavity 2 and Cavity 3. For the reasons argued above, these data are represented by a modified form of Eq. (13) giving:

$$Nu_{sh} = 0.25(Gr_{sh}Pr)^{1/4} + 0.057(Gr_{sh}Pr)^{1/3} \tag{20}$$

Fig. 5 compares the shroud heat transfer from the following test rigs: the disc and cone test rig (for a static shaft only); the narrow; and the wide annular gap test rig. The data are presented over the range of axial Reynolds numbers indicated in Table 1. Although not indicated here, the sense of shaft rotation does not have any systematic effect on the shroud Nusselt number. The results for Cavity 2 are shown and similar comments apply to Cavity 3. It is clearly seen that for $Gr_{sh} > 2\times10^8$, the shroud Nusselt number for the larger annular gap between shaft and disc bore is greater than that for the narrow annular gap. As noted by Long et al. (in press) there are also differences in the measured values of tangential velocity (albeit at lower radii than the shroud). These differences are attributed to the influence of the throughflow on the cavity flow. The narrow annular gap between shaft and disc bore would appear to attenuate the influence of the throughflow and this reduces the heat flux, and since T_{in} (which is unaffected) is used as the reference temperature to define the Nusselt number from the shroud, Nu_{sh} is reduced.

This explanation does however, lead to an inconsistency with the measurements on the shroud of the disc and cone rig. From Fig. 5 the shroud heat transfer for the disc and cone rig, with a restriction in the bore diameter immediately downstream of the cavity appears to be greater than that measured in the narrow annular gap test rig. Following the argument advanced above the restriction would be expected to have the reverse effect. This apparent contradiction may be explained by two-dimensional conduction effects which were not accounted for in the analysis of the shroud heat transfer data (Eq. (5) implies one-dimensional heat conduction) in the disc and cone rig. The presence of the cone immediately next to the shroud would be

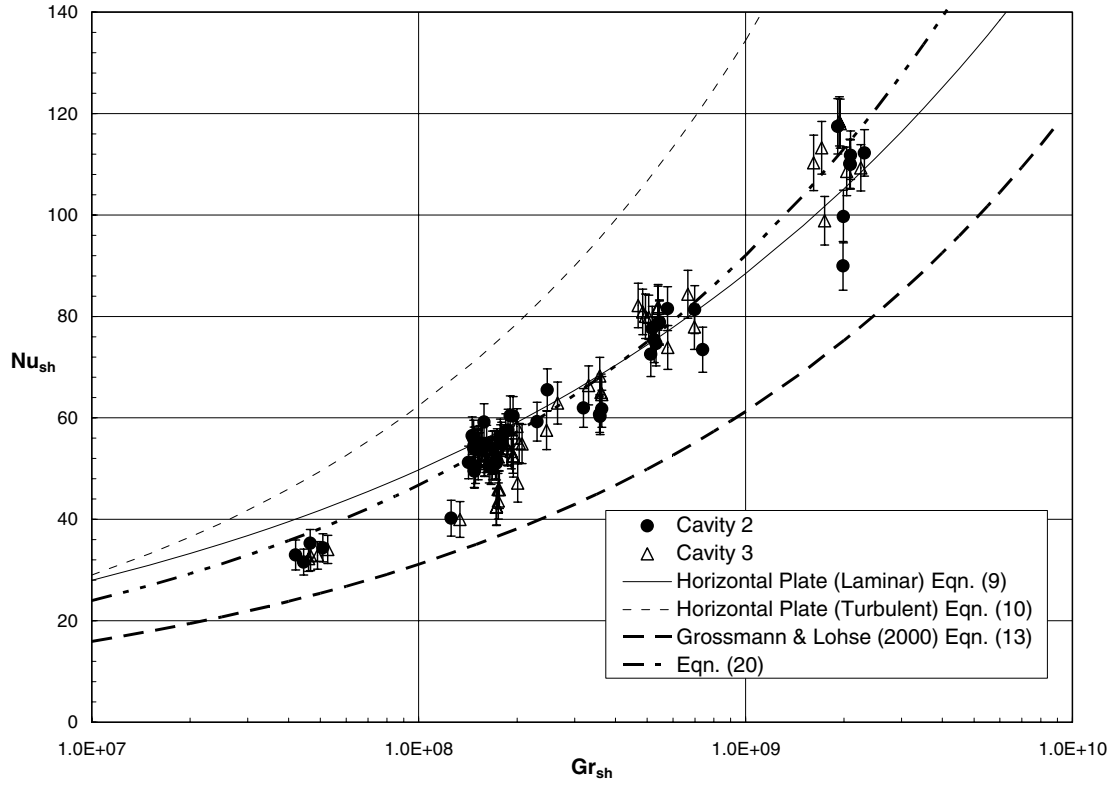

Fig. 4. Variation of shroud Nusselt number with Grashof number in both Cavity 2 and Cavity 3 for $d_h/b = 0.164$; $4.1 \times 10^4 < Re_z < 2.0 \times 10^5$; $0.27 < Ro < 5.8$. Uncertainty bars represent values calculated using Eq. (8) and Table 3.

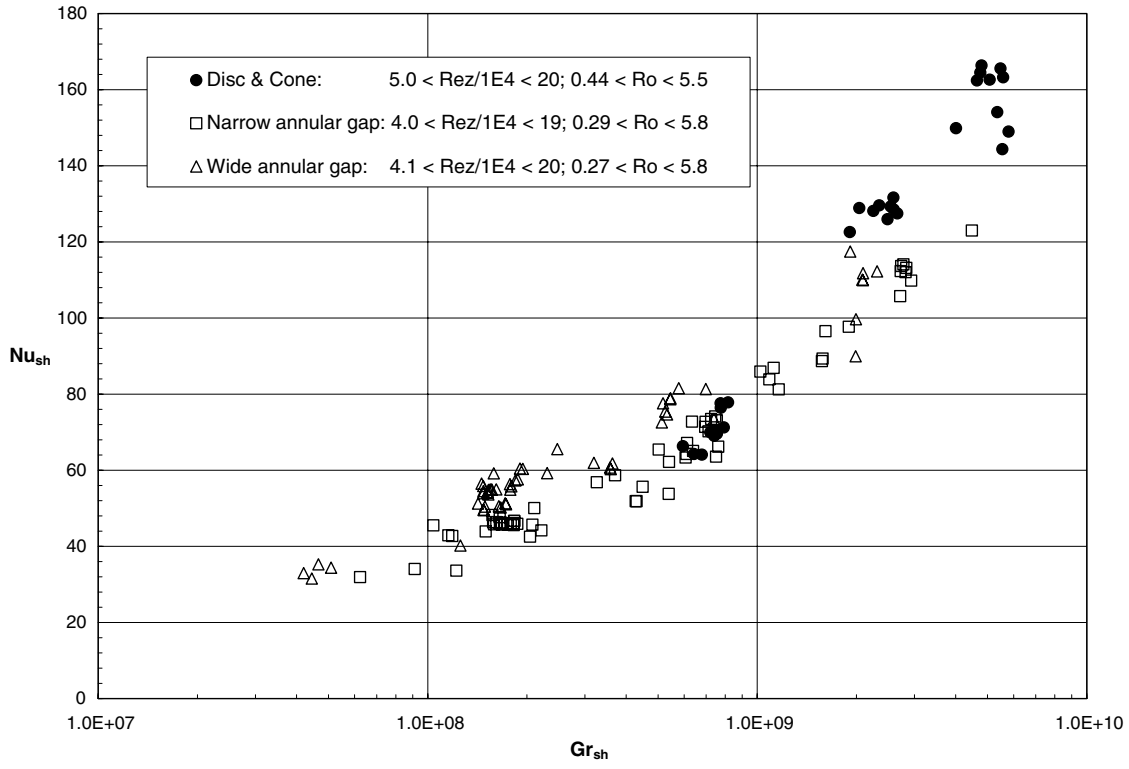

Fig. 5. Variation of shroud Nusselt number with Grashof number in Cavity 2. Comparison between results for the different configurations of test rig investigated.

expected to affect conduction paths inside the shroud and to a certain extent invalidate the assumption of one dimensional conduction. A two-dimensional conduction solution for the shroud of the disc and cone rig was not possible due to insufficient boundary conditions. The value of heat flux obtained from Eq. (5), should therefore overestimate the actual heat flux and this appears to be consistent with the data. There is no cone assembly in either the narrow or wide annular gap test rigs so these data are unlikely to be affected by two-dimensional conduction paths.

From the foregoing it is clear that heat transfer from a peripheral shroud is governed by free convection where the buoyancy force is generated from rotationally induced forces. It is also instructive to examine the heat transfer data from the *cone* surface itself (rather than the shroud) to see if this too behaves in this fashion. A clue to suggest that this behaviour does occur on the cone can be found in the form of correlation of the local Nusselt numbers (Alexiou et al., 2000). These measurements were made with a two-dimensional conduction solution of the cone surface. For $Ro < 3.5$, the local Nusselt numbers for the cone are correlated by:

$$Nu = 0.0243 Re_z^{0.086} \{Re_\phi^2 \beta \Delta T\}^{0.326} (r/b)^{-1.89} \{(b/r) - 1\}^{-0.022} \quad (21)$$

This indicates that the dependence on the axial Reynolds number is small and also that the Nusselt numbers are related to the product $Re_\phi^2 \beta \Delta T$, which is a Grashof number. The exponent to this term is very close to the value associated with turbulent free convection ($n = 1/3$). So it would appear that the heat transfer from a heated, rotating internal conical surface in the presence of axial throughflow may also behave as free convection from horizontal plate. This is confirmed in Fig. 6 which shows the variation of average Nusselt number with Grashof number obtained from tests on the cone. The length scales used to define both Gr_{sh} and Nu_{sh} are, as before, the ratio of exposed area to the perimeter (although, for turbulent free convection the choice of length scale for Nu and Gr is irrelevant, providing of course that the same length scale is used for both groups). The data are grouped into ranges of a buoyancy number, Bo, as indicated in the legend. This is adapted from the conventional definition ($=Gr/Re^2$) used in non-rotating systems to assess the relative contributions of free and forced convection. For a rotating cavity with an axial throughflow and a heated cone, the equivalent definition is taken as:

$$Bo = Re_\phi^2 \beta \Delta T / Re_z^2 \quad (22)$$

where ΔT is taken as the average cone surface to air inlet temperature difference.

Due to the relatively complex geometry involved here, the absolute values may not be entirely correct. But a value of $Bo \gg 1$ generally implies that free convection dominates; a value of $Bo \ll 1$ implies that forced convection dominates. Also shown in Fig. 6 are the curves for turbu-

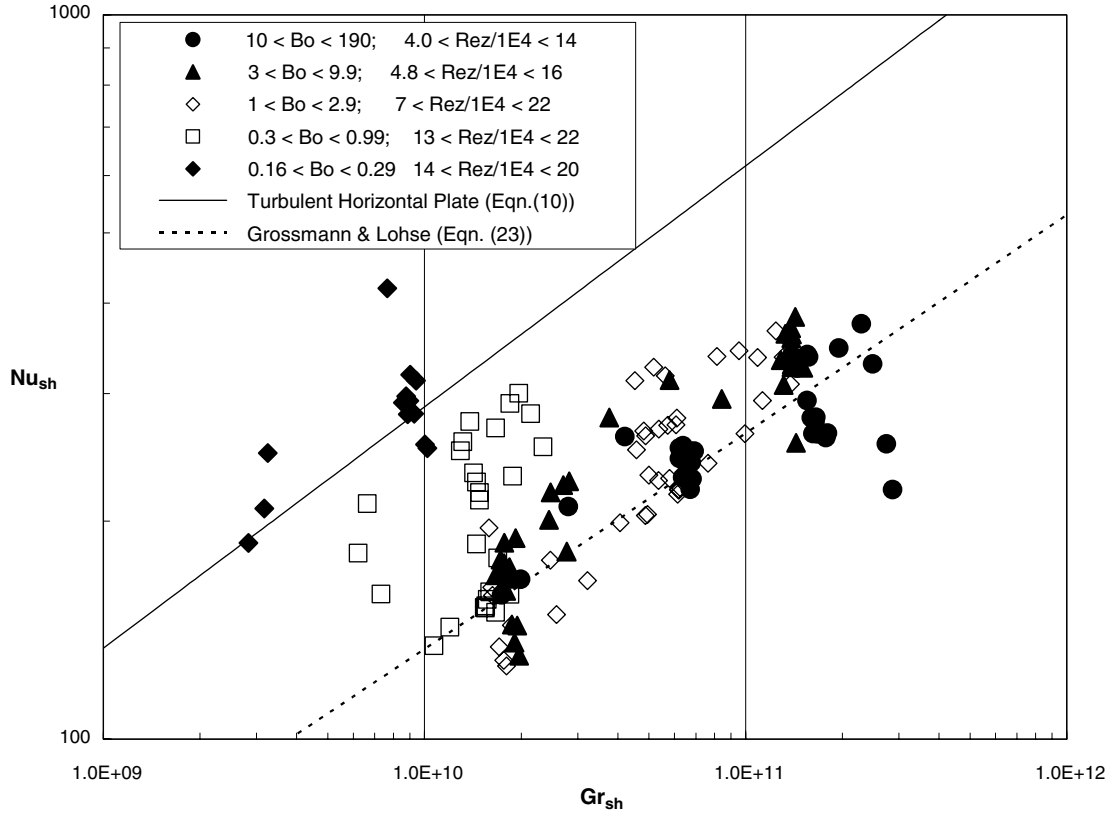

Fig. 6. Variation of Nusselt number with Grashof number for the internal surface of the cone in the disc and cone test rig.

lent free convection from a horizontal surface (Eq. (10)) and the Grossmann and Lohse correlation using the value of $(b - a)$ evaluated at the midpoint of the cone as the characteristic length scale. This gives:

$$Nu_{sh} = 0.205(Gr_{sh}Pr)^{1/4} + 0.038(Gr_{sh}Pr)^{1/3} \quad (23)$$

These data are also for tests with a static shaft, a co-rotating shaft and a contra rotating shaft. In addition, tests were also conducted with different values of mass flow extracted through the holes in the shaft. For the data here this varied in the range of 10–80% of the axial throughflow and this may account for the scatter in the data at large values of Bo and similar values of Gr_{sh}. As previously noted, and in particular since the geometry now being considered is now much more complex than an annular cavity, the prefactors in Eq. (23) are not expected to be the correct values. However, the curve does serve as a useful reference for Rayleigh–Bénard convection. As can be seen, for $1 < Bo < 190$, the experimental data show some similarity with the curve for Rayleigh–Bénard convection. As the buoyancy number is reduced beyond $Bo < 1$ there is a departure from this behaviour and it appears that Nu_{sh} is independent of the Grashof number. This is to be expected due to the more dominant influence of the axial throughflow on the cone heat transfer at small values of buoyancy number. In this region, the heat transfer from the cone is expected to be influenced by forced convection effects and Eq. (23) is not valid. The curve for turbulent free convection from a horizontal plate predicts values of shroud Nusselt number much greater than those measured. Although it is plausible that this correlation could predict the heat transfer from the cone, it does involve knowing the cavity air temperature T_{cav} and as previously noted this may not represent the physics of the flow in the outer part of the cavity.

6. Conclusions

This paper has presented measurements of shroud heat transfer tests carried out on a heated multiple cavity test rig. This experimental test rig is designed to be a 70% full scale replica of a high pressure compressor internal air system. Three different configurations of the test rig have been investigated. In one, the rig comprised two cylindrical cavities and a cone, the direction and speed of rotation of the central drive shaft could also be varied. In the other two, the rig comprised four identical cylindrical cavities and a non-rotating shaft. The difference between these two was in the annular gap between the shaft and the discs. For the narrow annular gap, $d_h/b = 0.092$ and for the wide annular gap $d_h/b = 0.164$.

Measurements of heat transfer were made using surface temperatures and a conduction solution method. These were carried out for a range of non-dimensional conditions that are representative of those found inside an engine.

The heat transfer from the shroud is seen to be governed by rotationally-induced free convection and depends only on the shroud Grashof number. The flow rate of the axial throughflow has little or no consistent effect on the shroud heat transfer. Although the cavity air temperature was not measured in these tests, earlier work where it was, demonstrated the principle that the shroud Nusselt number may be predicted from modified established correlations for free convection from a horizontal plate in a gravitational field. This modification takes the form of replacing the gravitational acceleration with the centripetal term and uses the cavity air temperature, not the inlet temperature. The current data are consistent with this and it is expected that if the cavity temperature was known, then it is possible that the shroud Nusselt numbers could be predicted from the free convection correlations. However, any such agreement is considered to be fortuitous and not be representative of the physical mechanisms of the flow in the outer part of the cavity. Instead, it is suggested that simple modifications are made to a correlation for Rayleigh–Bénard convection in a stationary enclosure. This does not require knowledge of the cavity temperature. It is shown that adjustment of the prefactors in this correlation gives an acceptable fit to the experimental data. Further work is required to establish how cavity geometry and disc heating affect this correlation.

There is a difference in the Nusselt numbers between the test rigs with the narrow and wide annular gaps between shaft and disc bores. The values of Nu_{sh} from $d_h/b = 0.164$ are greater than those for $d_h/b = 0.092$. This difference is attributed to the greater influence of the throughflow on the cavity air when the annular gap is increased. There is also some evidence to suggest that the heat transfer from the inside of a rotating conical surface exposed to axial throughflow can be predicted using a Rayleigh–Bénard correlation, providing the Buoyancy number is large enough, $Bo > 1$ in the data shown here.

Acknowledgements

The authors express their thanks to the following organisations that have supported this research work: The Engineering and Physical Sciences Research Council, Rolls-Royce Plc, the European Union and participating companies in the 4th and 5th Framework of the BRITE-Euram scheme of the European Union. We are also grateful to two former colleagues: Dr. Alex Alexiou, now at the Technical University of Athens, and Mr. Nicholas Miché, now at the University of Brighton, for their help with the experimental work. Finally, we thank Prof. J.M. Owen of Bath University for his critical but constructive comments on earlier versions of this paper.

References

Alexiou, A., 2000. Flow and heat transfer in gas turbine H.P. compressor internal air systems. D.Phil. thesis, School of Engineering, University of Sussex, UK.

Alexiou, A., Hills, N.J., Long, C.A., Turner, A.B., Millward, J.A., 2000. Heat transfer in high pressure compressor internal air systems: a

rotating disc-cone cavity with axial throughflow. International Journal of Experimental Heat Transfer 13, 299–328.

Burkhardt, C., Mayer, A., Reile, E., 1992. Transient thermal behaviour of a compressor rotor with axial cooling air flow and co-rotating or contra-rotating shaft. AGARD-CP-527, pp. 21-1–21-9.

Farthing, P.R., Long, C.A., Owen, J.M., Pincombe, J.R., 1992. Rotating cavity with axial throughflow of cooling air: heat transfer. ASME, Journal of Turbomachinery 114, 229–236.

Grossmann, S., Lohse, D., 2000. Scaling in thermal convection: a unifying theory. Journal of Fluid Mechanics 407, 27–56.

Howell, J.R., 1982. A Catalog of Radiation Configuration Factors. McGraw-Hill Book Company., New York.

King, M.P., Wilson, M., Owen, J.M., 2005. Rayleigh–Bénard convection in open and closed rotating cavities. Paper No. GT2005-68948, Presented at the ASME Turbo Expo, Reno, Nevada, USA.

Lancel, J., 2002. Analysis and test of a centrifugal compressor. D.Phil. Thesis, School of Engineering and Information Technology, University of Sussex, UK.

Lloyd, J.R., Moran, W.R., 1974. Natural convection adjacent to horizontal surfaces of various planforms. ASME Paper 74-WA/HT-66.

Long, C.A., 1985. The effect of thermocouple disturbance errors on the measurement of local heat transfer coefficients. Proceedings of Test and Transducer Conference, Wembley, London 3, 73–104.

Long, C.A., 1994. Disc heat transfer in a rotating cavity with an axial throughflow of cooling air. International Journal of Heat and Fluid Flow 15, 307–316.

Long, C.A., 1999. Essential Heat Transfer. Longman, London.

Long, C.A., Tucker, P.G., 1994. Shroud heat transfer measurements from a rotating cavity with an axial throughflow of air. ASME, Journal of Turbomachinery 116, 525–534.

Long, C., Alexiou, A., Smout, P.D., 2003. Heat transfer in H.P. Compressor internal air systems: measurements from the peripheral shroud of a rotating cavity with axial throughflow. In: The Second International Conference on Heat Transfer, Fluid Mechanics and Thermodynamics, Victoria Falls, Zambia, Presented at HEFAT 2003, Paper No. LC1.

Long, C.A., Miché, N.D.D., Childs, P.R.N., in press. Flow measurements inside a heated multiple rotating cavity with axial throughflow. International Journal of Heat and Fluid Flow. doi:10.1016/j.ijheatfluidflow.2007.04.010.

Rolls-Royce, 2005. The Jet Engine. Rolls-Royce Publications.

Sun, Z., Kilfoil, A., Chew, J.W., Hills, N.J., 2004. Numerical simulation of natural convection in stationary and rotating cavities Paper No. GT2004-53528, Presented at the ASME Turbo Expo, Vienna, Austria.

Tian, S. Tao, Z, Ding, S., Xu, G., 2004. Investigation of flow and heat transfer instabilities in a rotating cavity with axial throughflow of cooling air, Paper No. GT2004-53525, Presented at the ASME Turbo Expo, Vienna, Austria.

Touloukian, Y.S., Liley, P.E., Saxena, S.C., 1970a. Thermophysical properties of matterThermal Conductivity of Nonmetallic Liquids and Gases, vol. 3. IFI/Plenum, New York.

Touloukian, Y.S., Liley, P.E., Saxena, S.C., 1970b. Thermophysical properties of matterThermal Conductivity of Metallic Elements and Alloys, vol. 1. IFI/Plenum, New York.

Turner, A.B., 1970. Heat transfer instrumentation, AGARD-CP-73, Paper No. 5.

Vettori, R.L., Twilley, W.H., Stroup, D.W., 2001. Measurement techniques for low heat flux exposures to fire fighters protective clothing, United States Department of Commerce, National Institute of Standards and Technology, Report No. NISTIR 6750.